

Reliability and Failure Modes of Implant-Supported Y-TZP and MCR Three-Unit Bridges

Estevam Augusto Bonfante, DDS, MS, PhD candidate;^{*}

Paulo Guilherme Coelho, DDS, MS, BS, MSMtE, PhD;[†] Jose Manuel Navarro Jr, DDS, MS;[‡]

Luiz Fernando Pegoraro, DDS, PhD;[§] Gerson Bonfante, DDS, MS, PhD;[§] Van Purdy Thompson, DDS, PhD;[¶]

Nelson Renato Franç Alves Silva, DDS, MS, PhD^{**}

ABSTRACT

Purpose: Chipping within veneering porcelain has resulted in high clinical failure rates for implant-supported zirconia (yttria-tetragonal zirconia polycrystals [Y-TZP]) bridges. This study evaluated the reliability and failure modes of mouth-motion step-stress fatigued implant-supported Y-TZP versus palladium-silver alloy (PdAg) three-unit bridges.

Materials and Methods: Implant-abutment replicas were embedded in polymethylmethacrylate resin. Y-TZP and PdAg frameworks, of similar design ($n = 21$ each), were fabricated, veneered, cemented ($n = 3$ each), and Hertzian contact-tested to obtain ultimate failure load. In each framework group, 18 specimens were distributed across three step-stress profiles and mouth-motion cyclically loaded according to the profile on the lingual slope of the buccal cusp of the pontic.

Results: PdAg failures included competing flexural cracking at abutment and/or connector area and chipping, whereas Y-TZP presented predominantly cohesive failure within veneering porcelain. Including all failure modes, the reliability (two-sided at 90% confidence intervals) for a "mission" of 50,000 and 100,000 cycles at 300 N load was determined (Alta Pro, Reliasoft, Tucson, AZ, USA). No difference in reliability was observed between groups for a mission of 50,000. Reliability remained unchanged for a mission of 100,000 for PdAg, but significantly decreased for Y-TZP.

Conclusions: Higher reliability was found for PdAg for a mission of 100,000 cycles at 300 N. Failure modes differed between materials.

KEY WORDS: all-ceramic, fixed partial denture, mechanical testing, metal ceramic restoration, step-stress fatigue, Y-TZP

^{*}Department of Prosthodontics, Integrated Center for Research, Bauru School of Dentistry, University of São Paulo, Bauru, SP, Brazil; [†]assistant professor, Department of Biomaterials and Biomimetics, New York University School of Dentistry, New York, USA; [‡]private practice, Branemark Osseointegration Center, Centro Dental Humiaga, Canary Islands; [§]associate professor, Department of Oral Rehabilitation, Integrated Center for Research, Bauru School of Dentistry, University of São Paulo, Bauru, SP, Brazil; [¶]chairman, Department of Biomaterials, New York University School of Dentistry, New York, USA; ^{**}assistant professor, Department of Prosthodontics and the Department of Biomaterials and Biomimetics, New York University School of Dentistry, New York, USA

Reprint requests: Dr. Estevam A. Bonfante, Rua Vivaldo Guimarães 17-62, Jd. Ferraz, Bauru, SP 17012120, Brazil; e-mail: estevamab@gmail.com

Preliminary work presented at the IADR General Session in Toronto, July 2008.

© 2009, Copyright the Authors
Journal Compilation © 2009, Wiley Periodicals, Inc.

DOI 10.1111/j.1708-8208.2009.00156.x

INTRODUCTION

All-ceramic restorations have been extensively used by clinicians and dental laboratories because of their esthetically pleasant properties. Alumina and zirconia are the most common systems utilized for all-ceramic crowns and three-unit bridges.¹

From a mechanical standpoint, zirconia frameworks may be regarded as the most suitable for posterior regions^{2,3} when compared with other all-ceramic systems. Yttrium oxide is added (2–3% mol of Y₂O₃) to pure zirconia in order to stabilize the tetragonal phase at room temperature, generating a multiphase material suitable for clinical applications, that is, partially stabilized zirconia.⁴ The utilization of partially stabilized zirconia (yttria-tetragonal zirconia polycrystals, Y-TZP) in the areas of high tensile stresses such as gingival side of dental bridge connectors is indicated because of its

inherent ability to suppress crack propagation within its bulk and at the veneer-framework interface.³ Recently, technical complications such as chipping of the veneering porcelain has resulted in significantly higher failure rates than found for metal ceramic retainer restorations (MCR) in both tooth⁵ and implant-supported fixed partial dentures (FPD).⁶

Implant-supported prostheses have been shown to be successful for treating edentulous areas. For example, a recent study⁷ has demonstrated survival rates of 89.1% and 86.7%, after a 10-year evaluation for conventional (tooth supported) and implant-supported metal ceramic FPDs, respectively. However, the correlation between failure modes and survival rates of MCR and all-ceramic FPDs on implants is still not clear.

Considering that function, environment, and fabrication operations play a role in prosthesis clinical survival,⁸ initial conditions including choice of framework material and design should be controlled prior to investigations concerning the reliability of MCR or all-ceramic FPDs. It has been shown that changes in framework design as well as at the gingival embrasure alter the fracture resistance of all-ceramic three-unit FPDs.⁹⁻¹¹

Long-term clinical survival data and in vitro evaluations directly comparing veneered Y-TZP framework to MCR are still sparse. In one of the few in vitro investigations,¹² the effect of substructure properties on the longevity of porcelain-veneered four-layer models was investigated. These models consist of a flat layer of porcelain veneered onto a core and cemented on a dentin-like substrate made of composite with a similar modulus of elasticity to dentin. It was found that veneer porcelain placed on a low-modulus alloy (gold-infiltrated) was vulnerable to both occlusal surface contact damage and porcelain lower surface radial fracture. On the other hand, veneer porcelain applied on a higher-modulus substrate (palladium-silver alloy [PdAg]) fractured chiefly from occlusal surface damage. Fracture in the porcelain/Y-TZP system was limited to surface damage in the veneer layer, similar to that in the porcelain/palladium-silver system.¹² It was also demonstrated that the bulk fracture frequently observed in veneered alumina layers was not found for Y-TZP groups.

Despite the sparse and contradictory literature on this topic, observations have clearly demonstrated that for ceramic systems, the nature of substrate plays a significant role on the fracture modes and survival rates of ceramic restorations.¹³

This study compared the reliability and failure modes of implant supported three-unit Y-TZP and PdAg-supported FPDs, using controlled framework design and contour of veneering porcelain. Two research hypotheses were tested in this investigation: (1) Lower reliability is to be expected for veneered Y-TZP three-unit frameworks compared with veneered PdAg, and (2) different veneer fracture patterns are to be expected between groups as a result of the differing modulus of elasticity of the frameworks.

MATERIALS AND METHODS

Matrix for Specimen Production

Two implant-abutment replicas (Replica Snappy Abutment, Nobel Biocare, Gothenburg, Sweden) were embedded in polymethyl-methacrylate resin (Orthodontic Resin, Dentsply Caulk, Philadelphia, PA, USA) leaving 1 mm of implant-abutment replicas finishing line exposed above the potting surface (Figure 1, A and B). An implant locator was positioned in a surveyor to locate the implant-abutment replicas 19 mm apart from the center, representing the dimension of a missing first lower molar. The resin block with embedded implant-abutment replicas was used for the production of all

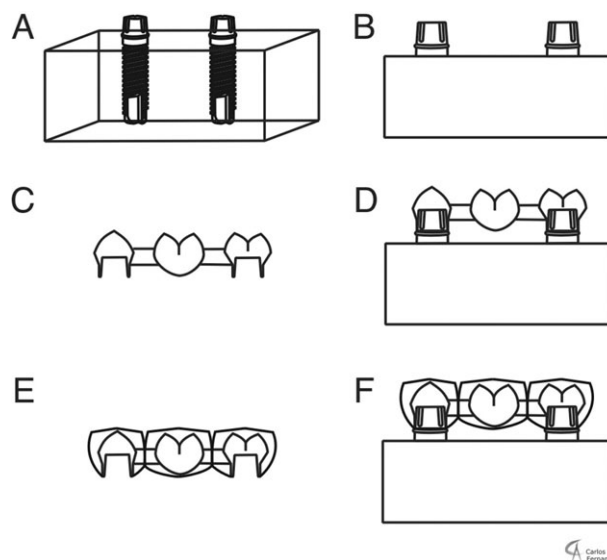


Figure 1 (A,B) Schematics of embedded implant analogues with cementable abutments. (C) Lab production of controlled shape yttria-tetragonal zirconia polycrystals and palladium-silver alloy frameworks used embedded analogues as a reference during construction and (D) for try-in and check of fit. (E) After veneering, (F) both groups presenting the same porcelain contour were cemented to embedded implants individually prepared for each tested bridge. 102 × 95 mm (300 × 300 DPI).

Y-TZP and PdAg frameworks. For mechanical testing, one individual block with embedded implant-abutment replicas for each bridge was produced to assure proper loading orientation and distribution.

Y-TZP Framework Fabrication

Y-TZP (LAVA, 3M-ESPE, St. Paul, MN, USA) frameworks were fabricated using the standard block with implant-abutment replicas for scanning procedures. The LAVA scanner consists of a noncontact optical scan system and a computer with the LAVA CAD Windows™-based software, which displays the model as a three-dimensional object. The scanning procedure took approximately 12 minutes. The CAD software designs an enlarged framework that is milled for 75 minutes from softer presintered blanks. The green state-machined frameworks ($n = 21$) underwent sintering (heating and cooling phases of approximately 8 hours) and attained their final dimensions, density, and final strength in a high-temperature (1,360°C–1,530°C; Figure 1, C and D) automated oven (LAVA Therm, 3M-Espe). The mean area of both distal and mesial connectors was 12 mm.²

PdAg Framework Fabrication

To obtain PdAg specimens of similar contour and design, an impression of one of the Y-TZP LAVA frameworks was made with vinyl polysiloxane impression material (Exafast Putty, GC-America Inc., Alsip, IL, USA) to serve as a key for wax up and subsequent casting in a PdAg alloy (Superior Plus, Jensen Industries, North Haven, CT, USA) of the PdAg frameworks. The casting procedure was performed following manufacturer's recommendations. The invested waxed pattern was burned out at 840°C and the alloy cast at 1,335°C, delivering a 1-unit casting (no welding or soldering). PdAg three-unit bridges ($n = 21$) of the same design and dimension of Y-TZP frameworks were fabricated.

Veneer Layer Application

For the LAVA group, frameworks were veneered with a 1.5 mm of feldspathic porcelain (Shade DA1, Lava Ceram, 3M ESPE, Seefeld, Germany), fired and glazed according to manufacturer instructions. PdAg frameworks were layered with two opaque pastes, a clear-translucent porcelain (Creation CC, Jensen Industries), and a glaze, each respectively fired according to manufacturer directions. The shape was defined by the use of

a silicon impression taken from a wax-up of the desired final contour of the bridges (Figure 1, E and F).

Mechanical Testing

Prior to mechanical testing, all bridges were cemented (RelyX Unicem, 3M-ESPE) to the implant-abutment replicas and incubated for 48 hours in water to allow hydration to the cement and resin block.

In order to test the bridges in a challenging scenario, mechanical testing was undertaken with all specimens held at a 30-degree axial inclination (Figure 2), with the indenter contacting the pontic lingual slope of the buccal cusp. The intent was to provide a bending component during loading. Three specimens of each group underwent single load to failure (SLF) testing, using a universal testing machine equipped with 6.25 mm diameter spherical tungsten carbide indenter and 10,000 N load cell at cross-head speed of 1 mm/min (INSTRON 5666 machine, Canton, MA, USA). The mean load to failure was calculated for each group. Based upon the mean load to failure, step-stress accelerated life testing profiles were determined. This fatigue testing approach consists of testing the samples at stress levels higher than use stress in order to facilitate failures in a timely manner. The results of these tests are then analyzed so that a profile of the failure behavior of the specimens at use stresses can be determined based on

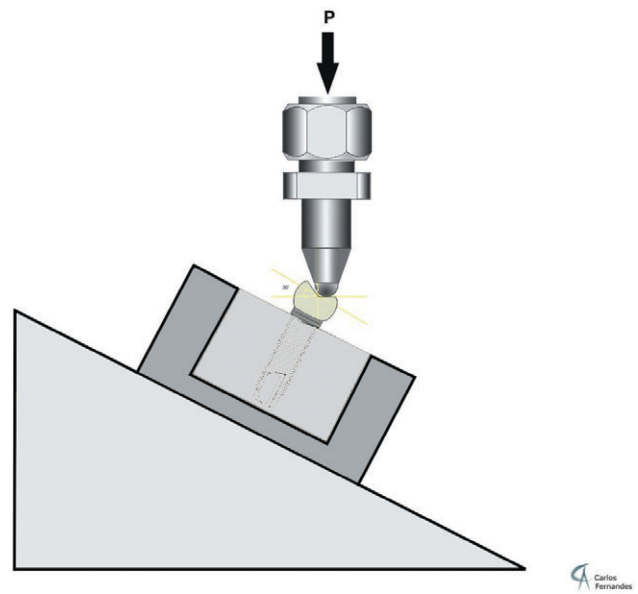


Figure 2 A 30-degree angled base was used to secure the holder with embedded implants and cemented bridges. An off-axis fatigue load (P) was applied on the pontic lingual slope of the buccal cusp. 77 × 72 mm (300 × 300 DPI).

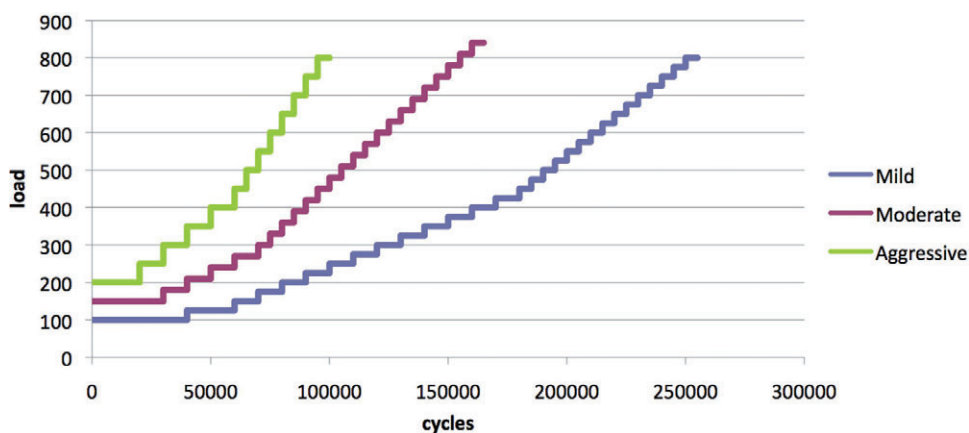


Figure 3 This chart shows the mild, moderate, and aggressive profiles used for accelerated fatigue testing of yttria-tetragonal zirconia polycrystals and palladium-silver alloy bridges. 117 × 52 mm (300 × 300 DPI).

the behavior of the samples at the accelerated stresses. The profiles were designated mild, moderate, and aggressive, with the number of specimens assigned to each group in approximately the ratio 3:2:1, respectively. Therefore, out of the 18 samples per group, nine were allocated for mild, six for moderate, and three for the aggressive profile. Mild, moderate, or aggressive profiles refer to the increasingly step-wise rapidness in which a specimen is fatigued to reach a certain level of load, meaning that specimens assigned to a mild profile will be cycled longer to reach the same load of a specimen assigned to either moderate or aggressive profiles (Figure 3). The mouth motion fatigue testing (where the indenter slides approximately 0.5 mm along the surface because of the slope presented by specimen angulation and anatomy) was then performed at 2 Hz using an electrodynamic fatigue testing machine (ELF 3300, EnduraTec Division, Bose Corporation, Minnetonka, MN, USA).

The specimens were evaluated at the completion of each fatigue step for crack evolution. Criteria used for failure were: delamination (framework exposure), cohesive fracture within veneering porcelain (chipping), cracks that extended to the framework (radial cracks), and catastrophic failure (bulk fracture).¹⁴ Based upon the step-stress distribution of the failures, use level probability Weibull curves (unreliability vs cycles) with use stress of 300 N and 90% two-sided confidence intervals were calculated and plotted (Alta Pro 7, ReliaSoft, Tucson, AZ, USA) using a power law relationship for damage accumulation. Reliability for a mission of 50,000 and 100,000 cycles at 300 N (90% two-sided confidence interval) was calculated for comparison between

the PdAg and Y-TZP groups. The Weibull modulus two-sided 90% confidence intervals were calculated using the Fisher Matrix method.

Representative failed samples were first inspected in polarized light (MZ-APO stereomicroscope, Carl Zeiss MicroImaging, Thornwood, NY, USA) and then gold sputtered (Emitech K650, Emitech Products Inc., Houston, TX, USA) followed by fractographic analysis using a scanning electron microscope (SEM) (Hitachi, Model 3500S, Osaka, Japan).

RESULTS

SLF and Reliability

The mean values obtained through SLF testing demonstrated significant difference ($p < .10$) between PdAg and Y-TZP groups (945 ± 200 N and 692 ± 83 N, respectively).

The use level probability Weibull plots at use stress of 300 N and 90% confidence interval for Y-TZP and PdAg revealed overlap of the confidence intervals, indicating no statistical difference ($p > .10$) between groups.¹⁵ Beta values of 2.08 (1.18–3.67) for Y-TZP and 0.55 (0.29–0.55) for PdAg showed that Y-TZP failures were influenced by fatigue and damage accumulation while strength was the main factor dictating the behavior for the PdAg group, not damage accumulation. Note that the beta value (called the Weibull shape factor) describes failure rate changes over time (beta < 1: failure rate is decreasing over time, commonly associated with “early failures” or failures that occur because of egregious flaws; beta ~1: failure rate that does not vary over time, associated with failures of a random nature;

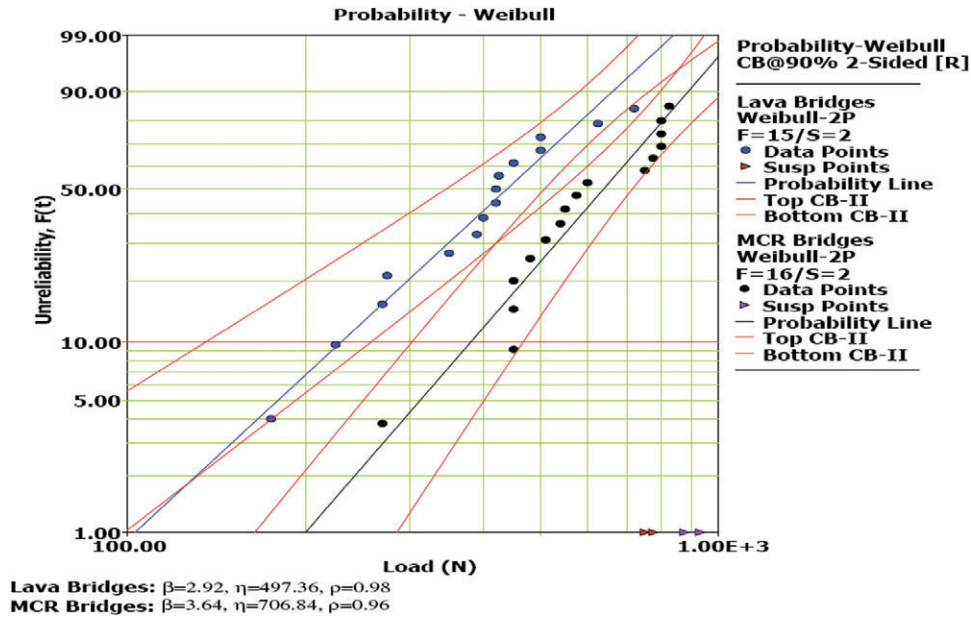


Figure 4 This figure shows a probability Weibull multi-plot (Unreliability vs Load) for metal ceramic retainer restoration (MCR) and yttria-tetragonal zirconia polycrystals (Y-TZP). Note that the characteristic strength (η) for palladium-silver alloy (706.8) is approximately 35% higher than Y-TZP (497.3). 88 × 57 mm (300 × 300 DPI). CB = Confidence Bounds; F = Failed; R = Reliability; S = specimens suspended; Susp = Suspended depicted in the graph.

beta > 1: failure rate is increasing over time, associated with failures related to damage accumulation).

The data was replotted according to the load at failure (assuming fatigue played little or no role in failure) in Figure 4 as a Weibull distribution (Weibull 7+, Reliasoft) for each group. The Weibull modulus for the PdAg group was $\beta = 3.64$ (2.60–5.11) and for the Y-TZP $\beta = 2.92$ (2.09–4.07). The characteristic strengths (η , which indicates the load at which 63.2% of the specimens of each group would fail) were PdAg = 706.8 N (631.0–791.8) and Y-TZP = 497.3 N (428.2–577.7), demonstrating statistically significant differences between groups ($p < .10$).

Table 1 lists the calculated reliability (two-sided 90% confidence intervals) for PdAg and Y-TZP groups. Reliability for completion of a mission of 50,000 cycles at 300 N showed overlap between groups, indicating no significant difference. However, difference was observed (no overlap of upper and lower limits) for completion of a mission of 100,000 cycles at this same load), demonstrating statistically significant decrease in reliability for Y-TZP compared with the PdAg group.

Failure Modes for Y-TZP

The predominant failure mode observed in this group was cohesive within the veneering porcelain at the pontic area ($n = 14, 71\%$). On the remaining four

specimens (39%), delamination of the veneer porcelain extended almost all the way to the core material. SEM analysis revealed fractographic markings depicting hackles, and wake hackles that allowed determination of the fracture origin, that is, the indentation area (Figure 5). Note that hackles are lines on the surface running in the local direction of cracking, separating parallel, but noncoplanar portions of the crack surface. When a hackle encounters a pore or any singularity, the crack proceeds along either side of the void and eventually reforms a continuous crack front on the other side. As the crack advances along the sides of the pore, however, it continues on slightly different planes. This causes a surface irregularity that leaves a trail (wake) emanating from the pore, called wake hackle.¹⁶

Fractographic analysis (Figure 5) also showed that the crack front propagated in different directions, but mainly toward margins of the veneering porcelain chip. No Y-TZP framework fractures were detected.

Failure Modes for PdAg

The predominant failure mode observed was flexure cracks at the connector area competing with either cohesive failure within veneering porcelain ($n = 11, 61\%$) or failure to the metallic core ($n = 7, 39\%$). SEM analysis showed the extension of cohesive failure at the connector area as well as quasiplastic deformation at the

TABLE 1 Reliability for Completion of a Mission of 50,000 Cycles at 300 N Is Not Significant for Both Groups. Calculation of a Mission of 100,000 Cycles at the Same Load Showed the Same Reliability for palladium-silver (PdAg) While it Decreased for Yttria-Tetragonal Zirconia Polycrystals (Y-TZP) Bridges

Output	Y-TZP (Lava-Espe)	PdAg (Jensen Ind.)
Mission of 50,000 cycles at 300 N		
Upper limit	0.96	0.98
Reliability	0.87	0.95
Lower limit	0.6	0.84
Mission of 100,000 cycles at 300 N		
Upper limit	0.71	0.98
Reliability	0.55*	0.95*
Lower limit	0.35	0.84

*Significant difference ($p < .05$).

113 × 62 mm (300 × 300 DPI).

indentation area (Figure 6). For detailed characterization of the flexure cracks, representative specimens were embedded in epoxy resin (Epofix Resin, Struers, Ballerup, Denmark), sectioned, and serially polished from mesial to distal (sagittal plane reference) and parallel to abutment axial direction. This permitted sequential light microscopy analysis of crack location and direction. Crack initiation sites at the abutment margin were detected and followed a path toward the indenter site. Crack zones (inner cone cracks from hydraulic pumping,¹⁷ were also detected in the connector region (Figure 6). No framework fractures were observed.

DISCUSSION

Information regarding a variety of Y-TZP FPDs systems has been reported in both clinical^{5,6,18,19} and in vitro^{3,20} studies. The MCR has been considered the “gold-standard,” despite the paucity of clinical data.²¹ We compared Y-TZP with PdAg, a common type of MCR alloy, utilizing a testing scenario with standardized dimensions of the framework, and veneering ceramics. Implant-supported MCR bridges have a significantly lower 5-year success when compared with conventionally supported bridges.⁷ The most frequent complication of Y-TZP FPDs is cohesive failure within veneering porcelain and it is also more common in implant supported⁶ when compared with conventionally supported.^{18,19,22} Thus, laboratory mechanical testing of implant-supported PdAg and Y-TZP FPDs should provide a sound basis to project the clinical reliability of these systems.

In this investigation, bridges were tested at a 30° angle on the buccal cusp of the pontic and thus challenged the ability of the veneer core system to withstand both vertical and lateral flexure. SEM of chipped MCR samples did not disclose the same fractographic features observed in Y-TZP samples. Whereas the latter presented telltale indicators of crack direction in the veneering porcelain, such as hackles and wake hackles (Figure 5), the former disclosed obvious quasiplastic deformation in the indented area, but no such fractographic markings in the failed porcelain veneer (Figure 6). The PdAg veneering porcelain has a more coarse inclusion structure which may account for this observation.

With higher strength than previous all-ceramic materials,^{23,24} Y-TZP was introduced in dentistry as a structural ceramic with mechanical properties comparable with metals.^{1,8,14,25} However, the significantly lower reliability observed for Y-TZP compared with PdAg FPDs after completion of a mission of 100,000 cycles at 300 N (Table 1) suggests that material's properties other than strength play a role in its performance.

Modulus of elasticity, hardness, and toughness are also important predictors of reliability in core-veneered all-ceramic systems.¹⁴ However, these properties in both the PdAg and Y-TZP systems were sufficient to withstand fatigue as failure of the framework was not observed for either group. Thus, the lower reliability observed for the Y-TZP resulted mainly from veneering porcelain failure. This may be related to the very low thermal diffusivity of Y-TZP

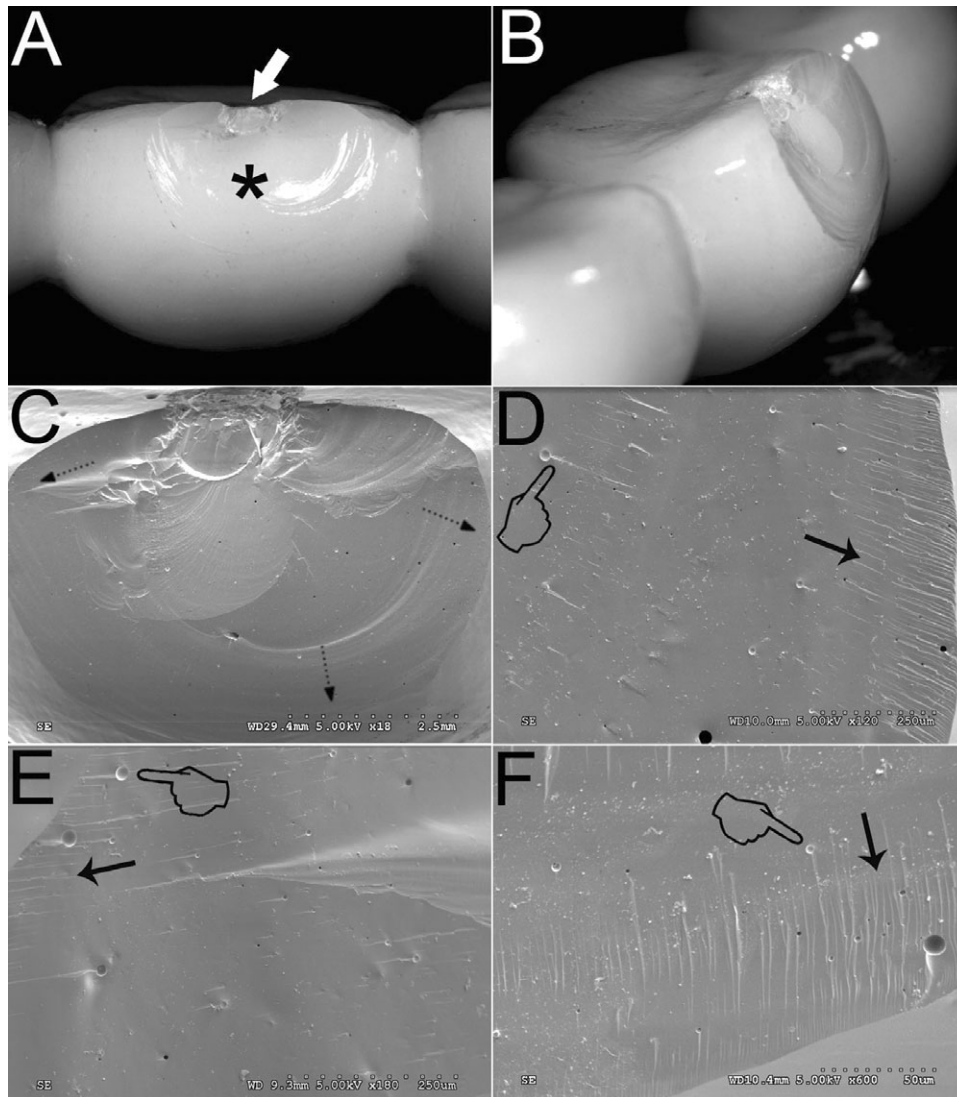


Figure 5 Yttria-tetragonal zirconia polycrystals bridge failed after fatigue. Light polarized microscopy shows (A) buccal view of indented occlusal area (*arrow*) and chipped veneering porcelain with no framework exposure (*asterisk*). (B) Proximal view of pontic depicts depth of porcelain cohesive failure. (C) A buccal scanning electron microscope low magnification view shows fractographic markings that indicate direction of crack propagation toward the margins (*dotted arrows*). Clockwise magnifications of these marginal areas (D, E, and F) show telltale fractographic markings such as hackles (*arrows*) and wake hackles (*pointers*) pointing crack direction toward the margins of fractured veneer. 143 × 164 mm (300 × 300 DPI).

($\sim 3 \text{ Wm/K}$)²⁶ as compared with PdAg ($\sim 100 \text{ Wm/K}$),²⁷ which will affect the rate of cooling of the veneering porcelain. This cooling rate difference may lead to different stress states in the two systems. The large chips observed for the Y-TZP veneer without exposure of the veneer core interface strongly suggest high residual stresses in the veneer.

The higher reliability (mission of 100,000 cycles at 300 N) of the PdAg bridges was a result of higher loads to initiate failures of veneering porcelain at the indenter that was commonly coupled with flexural cracks from the connector area. While indenter area-related cracks

may have been initiated at similar number of cycles for a given load compared with Y-TZP specimens, in the all-ceramic system they quickly lead to large chips (perhaps from residual stress) and connector area cracks were not often observed. We speculate that the lower modulus of PdAg frameworks (140 GPa vs 205 GPa for Lava) may have resulted in more flexing of the PdAg bridges during fatigue, especially at the gingival area of connectors, where tensile stresses are expected.¹¹ This likely resulted in flexural cracks, however, still occurring at stresses higher than those that resulted in large chips for the Y-TZP group.

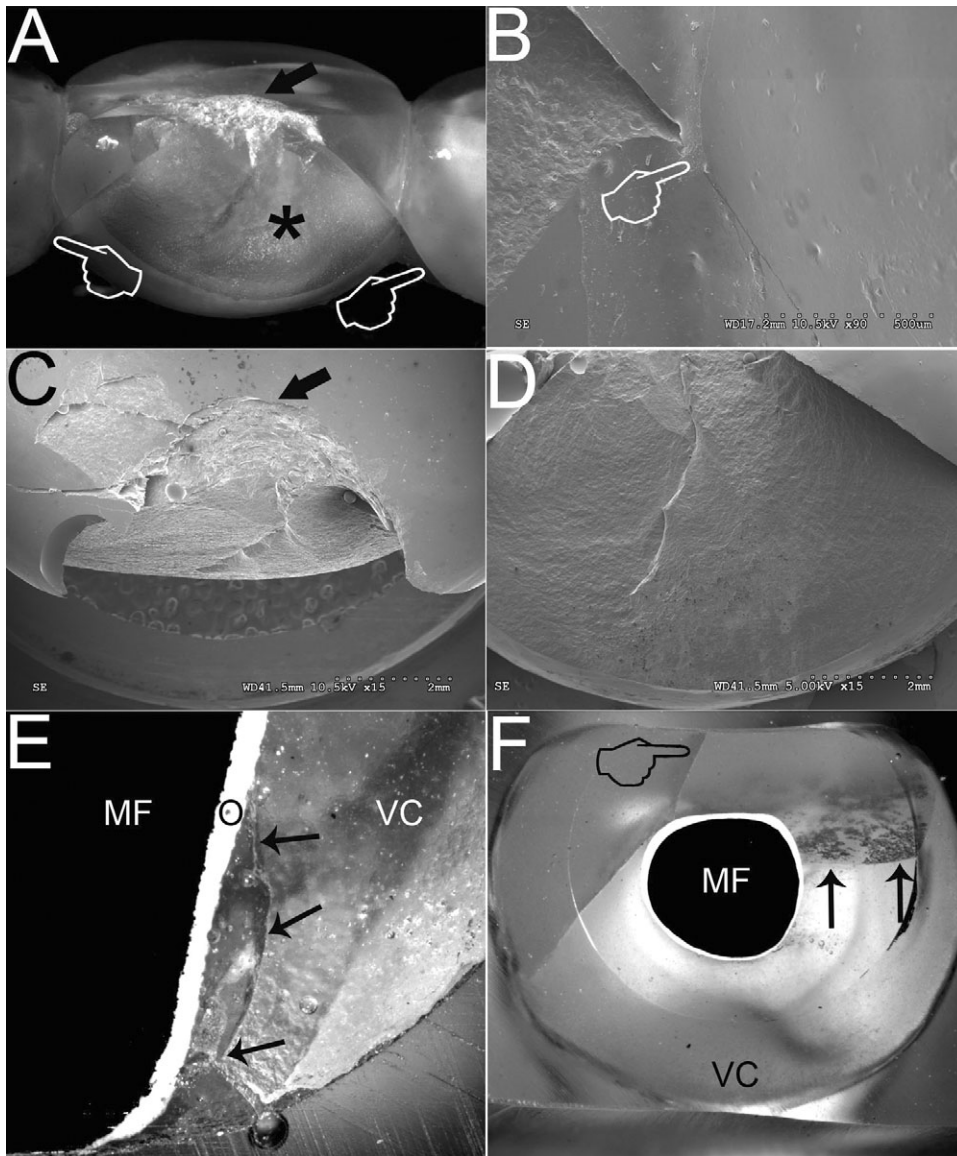


Figure 6 Palladium-silver alloy bridge sample after fatigue showing the two competing fracture modes: (A) polarized light microscopy depicting indented area (*arrow*), the two flexural cracks coming from mesial and distal abutments (*pointers*), and the cohesive failure of veneering porcelain on loaded lingual slope of the buccal cusp (*asterisk*). The scanning electron microscope micrographs show (B) magnification of distal pontic-abutment boundary where veneer cohesive failure and flexural crack line intersect, occlusal view (C) of indenter damage area, and (D) buccal view of chipped porcelain. (E) Mesio-distal sectioning of bridge embedded in epoxy resin shows, in light polymerized microscopy, the flexural crack at the abutment cervical margin (*arrows*) in its upward path toward indented area. Note that in connector area, (F) flexural crack (*arrows*) is accompanied by a radial crack that is deviated to lingual after contact with metal framework (MF). The dark spots above arrows represent entrapped water in the flexural crack. 143 × 172 mm (300 × 300 DPI). O = opaque layer; VC = veneering ceramics.

CONCLUSION

Y-TZP and PdAg FPDs demonstrated no difference in reliability for a mission of 50,000 cycles at 300 N. However, significant reduction in reliability was found for Y-TZP FPDs for a completion of a mission of 100,000 cycles at the same load. Thus, hypothesis 1, which postulated that lower reliability was to be

expected for Y-TZP FPDs compared with PdAg, was partially accepted. Failure modes were similar between groups, except for the additional competing flexural cracks observed in most PdAg bridges. Therefore, hypothesis 2, which postulated that different veneer failure modes would be evident for the framework materials, was also partially accepted. Future studies are needed, incorporating sliding contact fatigue associated

with different framework design in an attempt to improve the reliability of veneered Y-TZP systems.

ACKNOWLEDGMENTS

The authors are thankful to Capes Brazil (4695/06-2), 3M-ESPE, Marotta Dental Studio, and Jensen Industries for their support. A special acknowledgment goes to Dr. Carlos A.O. Fernandes (Federal University of Ceara, Fortaleza, Brazil) for the illustrative schematics on Figures 1 and 2.

REFERENCES

- Conrad HJ, Seong WJ, Pesun IJ. Current ceramic materials and systems with clinical recommendations: a systematic review. *J Prosthet Dent* 2007; 98:389–404.
- Raigrodski AJ. Contemporary materials and technologies for all-ceramic fixed partial dentures: a review of the literature. *J Prosthet Dent* 2004; 92:557–562.
- Studart AR, Filser F, Kocher P, Lüthy H, Gauckler LJ. Cyclic fatigue in water of veneer-framework composites for all-ceramic dental bridges. *Dent Mater* 2007; 23:177–185.
- Piconi C, Maccauro G. Zirconia as a ceramic biomaterial. *Biomaterials* 1999; 20:1–25.
- Sailer I, Feher A, Filser F, Gauckler LJ, Lüthy H, Hammerle CH. Five-year clinical results of zirconia frameworks for posterior fixed partial dentures. *Int J Prosthodont* 2007; 20:383–388.
- Larsson C, Vult von Steyern P, Sunzel B, Nilner K. All-ceramic two- to five-unit implant-supported reconstructions. A randomized, prospective clinical trial. *Swed Dent J* 2006; 30:45–53.
- Pjetursson BE, Brägger U, Lang NP, Zwahlen M. Comparison of survival and complication rates of tooth-supported fixed dental prostheses (FDPs) and implant-supported FDPs and single crowns (SCs). *Clin Oral Implants Res* 2007; 18:97–113.
- Rekow D, Thompson VP. Engineering long term clinical success of advanced ceramic prostheses. *J Mater Sci Mater Med* 2007; 18:47–56.
- Kokubo Y, Tsumita M, Sakurai S, Torizuka K, von Steyern PV, Fukushima S. The effect of core framework designs on the fracture loads of all-ceramic fixed partial dentures on posterior implants. *J Oral Rehabil* 2007; 34:503–507.
- Oh WS, Anusavice KJ. Effect of connector design on the fracture resistance of all-ceramic fixed partial dentures. *J Prosthet Dent* 2002; 87:536–542.
- Oh W, Gotzen N, Anusavice KJ. Influence of connector design on fracture probability of ceramic fixed-partial dentures. *J Dent Res* 2002; 81:623–627.
- Kim B, Zhang Y, Pines M, Thompson VP. Fracture of porcelain-veneered structures in fatigue. *J Dent Res* 2007; 86:142–146.
- Malament KA, Socransky SS. Survival of Dicor glass-ceramic dental restorations over 16 years. Part III: effect of luting agent and tooth or tooth-substitute core structure. *J Prosthet Dent* 2001; 86:511–519.
- Rekow D, Zhang Y, Thompson V. Can material properties predict survival of all-ceramic posterior crowns? *Compend Contin Educ Dent* 2007; 28:362–368; quiz 369, 386.
- Abernethy R. The new Weibull handbook. North Palm Beach, FL: Dr. Robert B. Abernethy, 2006.
- Quinn G. Fractography of ceramics and glasses. A NIST recommended practice guide; Special Publication 960-16. Washington DC: National Institute of Standards and Technology, 2007. Available at: <http://www.ceramics.nist.gov/pubs/practice.htm> (accessed May 30, 2007).
- Zhang Y, Song JK, Lawn BR. Deep-penetrating conical cracks in brittle layers from hydraulic cyclic contact. *J Biomed Mater Res B Appl Biomater* 2005; 73:186–193.
- Molin MK, Karlsson SL. Five-year clinical prospective evaluation of zirconia-based Denzir 3-unit FPDs. *Int J Prosthodont* 2008; 21:223–227.
- Tinschert J, Schulze KA, Natt G, Latzke P, Heussen N, Spiekermann H. Clinical behavior of zirconia-based fixed partial dentures made of DC-Zirkon: 3-year results. *Int J Prosthodont* 2008; 21:217–222.
- Kohorst P, Dittmer MP, Borchers L, Stiesch-Scholz M. Influence of cyclic fatigue in water on the load-bearing capacity of dental bridges made of zirconia. *Acta Biomater* 2008; 4:1440–1447.
- Pjetursson BE, Sailer I, Zwahlen M, Hammerle CH. A systematic review of the survival and complication rates of all-ceramic and metal-ceramic reconstructions after an observation period of at least 3 years. Part I: single crowns. *Clin Oral Implants Res* 2007; 18(Suppl. 3):73–85.
- Sailer I, Pjetursson BE, Zwahlen M, Hammerle CH. A systematic review of the survival and complication rates of all-ceramic and metal-ceramic reconstructions after and observation period of at least 3 years. Part II: fixed dental prostheses. *Clin Oral Implants Res* 2007; 18:86–96.
- Guazzato M, Proos K, Sara G, Swain MV. Strength, reliability, and mode of fracture of bilayered porcelain/core ceramics. *Int J Prosthodont* 2004; 17:142–149.
- Guazzato M, Proos K, Quach L, Swain MV. Strength, reliability and mode of fracture of bilayered porcelain/zirconia (Y-TZP) dental ceramics. *Biomaterials* 2004; 25:5045–5052.
- Manicone PF, Rossi Iommetti P, Raffaelli L. An overview of zirconia ceramics: basic properties and clinical applications. *J Dent* 2007; 35:819–826.
- Birkby I, Stevens R. Applications of zirconia ceramics. *Key Eng Mater* 1996; 122–124:527–552.
- O'Brien WJ. Biomaterials Properties Online Database. University of Michigan, Quintessence Publishing, 2002. Available at: <http://www.lib.umich.edu/dentlib/Dentaltables.html> (accessed May 13, 2008).

Copyright of Clinical Implant Dentistry & Related Research is the property of Wiley-Blackwell and its content may not be copied or emailed to multiple sites or posted to a listserv without the copyright holder's express written permission. However, users may print, download, or email articles for individual use.